

# Polymerization of MMA by oscillating zirconocene catalysts, diastereomeric zirconocene mixtures, and diastereospecific metallocene pairs

Yalan Ning, Megan J. Cooney, Eugene Y.-X. Chen \*

Department of Chemistry, Colorado State University, Fort Collins, Colorado 80523-1872, United States

Received 29 December 2004; revised 19 January 2005; accepted 24 January 2005

Available online 23 May 2005

## Abstract

Characteristics of methyl methacrylate (MMA) polymerization using oscillating zirconocene catalysts, (2-Ph-Ind)<sub>2</sub>ZrX<sub>2</sub> (X = Cl, 1; X = Me, 2), mixtures of *rac*- and *meso*-zirconocene diastereomers, (SBI)ZrMe<sub>2</sub> [3, SBI = Me<sub>2</sub>Si(Ind)<sub>2</sub>] and (EBI)ZrMe<sub>2</sub> [4, EBI = C<sub>2</sub>H<sub>4</sub>(Ind)<sub>2</sub>], as well as diastereospecific metallocene pairs, *rac*-4/Cp<sub>2</sub>ZrMe<sub>2</sub> (5) and *rac*-4/CGCTiMe<sub>2</sub> [6, CGC = Me<sub>2</sub>Si(Me<sub>4</sub>C<sub>5</sub>)(*t*-BuN)], are reported. MMA polymerization using the chloride catalyst precursor 1 activated with a large excess of the modified methyl aluminoxane is sluggish, uncontrolled, and produces atactic PMMA. On the other hand, the polymerization by a 2/1 ratio of 2/B(C<sub>6</sub>F<sub>5</sub>)<sub>3</sub> or 2/Ph<sub>3</sub>CB(C<sub>6</sub>F<sub>5</sub>)<sub>4</sub> is controlled and produces syndiotactic PMMA. Mixtures of diastereomeric *ansa*-zirconocenes 3 or 4 containing various *rac*/*meso* ratios, when activated with B(C<sub>6</sub>F<sub>5</sub>)<sub>3</sub>, yield bimodal PMMA; this behavior is attributed to the *meso*-diastereomer that, in its pure form, affords bimodal, syndio-rich atactic PMMA. For MMA polymerization using diastereospecific metallocene pairs, *rac*-4/5 and *rac*-4/6, the isospecific catalyst site dominates the polymerization events under the conditions employed in this study, and the aspecific and syndiospecific sites are largely nonproductive, thereby forming only highly isotactic PMMA.  
© 2005 Elsevier B.V. All rights reserved.

**Keywords:** Metallocene catalysts; Oscillating catalysts; MMA polymerization; Tacticity; Diastereomers; Stereospecific polymerization

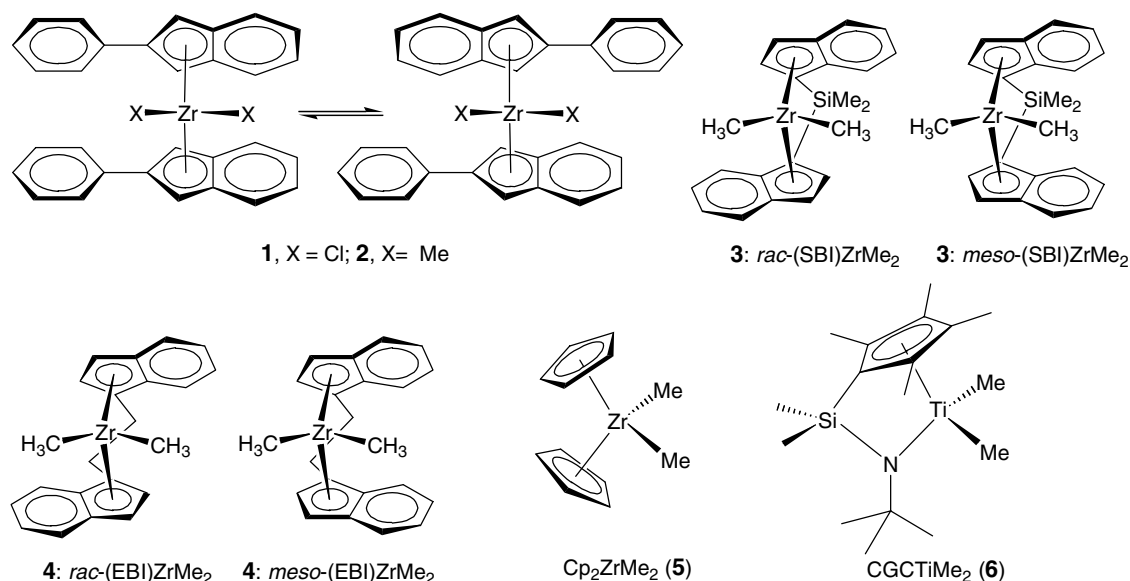
## 1. Introduction

A growing number of publications have been devoted to the investigation of the polymerization of methyl methacrylate (MMA) by group 4 metallocene and related catalysts; such complexes used for these studies have included achiral zirconocenes [1], chiral *ansa*-zirconocenes [2], achiral titanocenes [3], chiral *ansa*-titanocenes [4], half-sandwich titanium complexes [5], and constrained geometry titanium and zirconium complexes [6]. Furthermore, this polymerization has been examined computationally [7]. Three important attri-

butes of this polymerization explain why it has attracted increasing attention. First, there is a paradigm shift in terms of scientific curiosity on utilizing highly active, electro-deficient transition metal complexes for polymerization of polar functionalized alkenes. Second, group 4 metallocene complexes with considerably diverse structural motifs are readily, and in many cases commercially, available, thanks to comprehensive studies of their roles in coordination polymerization of nonpolar olefins. Third, these complexes, when used in a suitable initiating form, typically exhibit a high degree of control over polymerization, especially the stereochemistry of polymerization.

These recent advances [1–7], enabled by group 4 metallocene complexes, have resulted in the production of poly(methyl methacrylate) (PMMA) having various

\* Corresponding author. Tel.: +1 970 491 5609; fax: +1 970 491 1801.  
E-mail address: [eychen@lamar.colostate.edu](mailto:eychen@lamar.colostate.edu) (E.Y.-X. Chen).



Scheme 1.

stereo-microstructures, including atactic, isotactic, syndiotactic, as well as isotactic-*b*-syndiotactic stereodiblock and -multiblock PMMAs [5a]. We have been especially interested in the production of stereoblock PMMA microstructures using metallocene and related complexes through various unique strategies [2c,2g,5a]. In the present study, we became interested in unbridged bis(2-aryl-substituted indenyl) zirconocenes such as (2-Ph-Ind)<sub>2</sub>ZrCl<sub>2</sub>, which can oscillate between achiral (*meso*-like) and chiral (*rac*-like) configurations; when activated with methyl aluminoxane, they have been known to produce atactic-*b*-isotactic stereomultiblock polypropylene [8]. Thus, it is of interest to examine if such oscillating metallocene catalysts can also produce PMMA with stereomultiblock microstructures. Furthermore, polymerization of MMA using a mixture of *rac*- and *meso*-diastereomeric *ansa*-zirconocene catalysts may offer an intriguing possibility of generating stereoblock microstructures, provided that the diastereomers produce diastereomeric polymer chains and that the growing polymer chains can exchange infrequently between the two diastereomeric catalyst centers on the polymerization time scale. By the same reasoning, using diastereospecific catalyst pairs consisting of an isospecific/aspecific or isospecific/syndiospecific combination for MMA polymerization may also produce PMMA with unique stereomicrostructures. To address these fundamentally interesting questions, the present contribution investigates the MMA polymerization behavior of the following three classes of group 4 metallocenes (Scheme 1): oscillating catalysts 1 and 2, mixtures of diastereomeric *rac*- and *meso*-zirconocene catalysts 3 and 4, as well as diastereospecific catalyst pairs, *rac*-4/5, an isospecific/aspecific pair, and *rac*-4/6, an isospecific/syndiospecific pair.

## 2. Experimental

### 2.1. Materials and methods

All syntheses and manipulations of air- and moisture-sensitive materials were carried out in flamed Schlenk-type glassware on a dual-manifold Schlenk line, a high-vacuum line (10<sup>-5</sup>–10<sup>-7</sup> Torr), or in an argon-filled glovebox (<1.0 ppm oxygen and moisture). NMR-scale reactions (typically in a 0.02 mmol scale) were conducted in Teflon-valve-sealed J. Young-type NMR tubes. HPLC grade organic solvents were sparged with nitrogen during filling the solvent reservoir and then dried by passage through activated alumina (for Et<sub>2</sub>O, THF, and CH<sub>2</sub>Cl<sub>2</sub>) followed by passage through Q-5-supported copper catalyst (for toluene and hexanes) stainless steel columns. Benzene-*d*<sub>6</sub>, toluene-*d*<sub>8</sub>, and THF-*d*<sub>8</sub> were dried over sodium/potassium alloy and vacuum-distilled or filtered. NMR spectra were recorded on either a Varian Inova 300 (FT 300 MHz, <sup>1</sup>H; 75 MHz, <sup>13</sup>C; 282 MHz, <sup>19</sup>F) or a Varian Inova 400 spectrometer. Chemical shifts for <sup>1</sup>H and <sup>13</sup>C spectra were referenced to internal solvent resonances and are reported as parts per million relative to tetramethylsilane, whereas <sup>19</sup>F NMR spectra were referenced to external CFC1<sub>3</sub>.

Methyl methacrylate (MMA) was purchased from Aldrich Chemical Co.; MMA was first degassed and dried over CaH<sub>2</sub> overnight, followed by vacuum distillation; final purification involved titration with neat tri(*n*-octyl)aluminum to a yellow end point [9] followed by distillation under reduced pressure. The purified MMA was stored in a –30 °C glovebox freezer.

Tris(pentafluorophenyl)borane, B(C<sub>6</sub>F<sub>5</sub>)<sub>3</sub>, was obtained as a research gift from Boulder Scientific Co.

and further purified by recrystallization from hexanes at  $-35\text{ }^{\circ}\text{C}$ . Triisobutylaluminum-modified methylalumoxanes (MMAO) was purchased from Azko-Nobel, whereas  $\text{Ph}_3\text{CB}(\text{C}_6\text{F}_5)_4$  was prepared according to the literature procedure [10]. Tris(pentafluorophenyl)alane,  $\text{Al}(\text{C}_6\text{F}_5)_3$ , as a 0.5 toluene adduct based on the elemental analysis for the vacuum-dried sample, was prepared from the exchange reaction of  $\text{B}(\text{C}_6\text{F}_5)_3$  and  $\text{AlMe}_3$  in a 1:3 toluene/hexanes solvent mixture in quantitative yield according to the literature procedure [11], which is the modified synthesis of the alane first disclosed by Biagini et al. [12]. Extra caution should be exercised when handling this material because of its thermal and shock sensitivity.

Literature procedures were employed for the preparation of the following metallocene complexes:  $(2\text{-Ph-Ind})_2\text{ZrX}_2$  ( $\text{X} = \text{Cl}$ , **1**;  $\text{X} = \text{Me}$ , **2**) [13], *rac*-(SBI)ZrMe<sub>2</sub> [*rac*-**3**, SBI =  $\text{Me}_2\text{Si}(\text{Ind})_2$ ] [14], *rac*-(EBI)ZrMe<sub>2</sub> [*rac*-**4**, EBI =  $\text{C}_2\text{H}_4(\text{Ind})_2$ ] [15],  $\text{Cp}_2\text{ZrMe}_2$  (**5**) [16], and CGC-TiMe<sub>2</sub> [**6**, CGC =  $\text{Me}_2\text{Si}(\text{Me}_4\text{C}_5)(t\text{-BuN})$ ] [17]. A diastereomeric mixture of *rac*- and *meso*-(SBI)ZrMe<sub>2</sub> was synthesized according to Herrmann's procedures [18], followed by methylation with MeMgBr. The *meso*-enriched diastereomeric mixture of *rac*- and *meso*-(EBI)ZrMe<sub>2</sub> was obtained by Resconi's improved, two-step synthesis [19]. Crystalline fractions of (SBI)ZrMe<sub>2</sub> containing various *rac/meso* ratios were collected by fractional recrystallization of the diastereomeric mixture from a toluene/hexanes mixture at  $-35\text{ }^{\circ}\text{C}$ . Spectroscopically pure *meso*-(SBI)ZrMe<sub>2</sub> and *meso*-(EBI)ZrMe<sub>2</sub> fractions were obtained from the sixth crystalline fraction of the recrystallization. The corresponding active cationic species generated from the abstractive reactions of the metallocene dimethyl complexes with  $\text{M}(\text{C}_6\text{F}_5)_3$  ( $\text{M} = \text{B}, \text{Al}$ ) are known: *rac*-(SBI)ZrMe<sup>+</sup>MeM(C<sub>6</sub>F<sub>5</sub>)<sub>3</sub><sup>-</sup> [**20**], *rac*-(EBI)ZrMe<sup>+</sup>MeM(C<sub>6</sub>F<sub>5</sub>)<sub>3</sub><sup>-</sup> [**2a**, **20**],  $\text{Cp}_2\text{ZrMe}^+\text{MeB}(\text{C}_6\text{F}_5)_3^-$  [**21**], and CGCTiMe<sup>+</sup>MeB(C<sub>6</sub>F<sub>5</sub>)<sub>3</sub><sup>-</sup> [**22**]; in situ generation of the cationic species derived from the oscillating metallocene **2** is described as follows.

## 2.2. Reaction of $(2\text{-Ph-Ind})_2\text{ZrMe}_2$ and $\text{B}(\text{C}_6\text{F}_5)_3$

$(2\text{-Ph-Ind})_2\text{ZrMe}_2$  (0.02 mmol),  $\text{B}(\text{C}_6\text{F}_5)_3$  (0.02 mmol), and  $\sim 0.7\text{ mL}$  toluene-*d*<sub>8</sub> were mixed in a 4-mL vial, and the resulting orange yellow solution was loaded into a J. Young NMR tube via pipette. The mixture was allowed to react at ambient temperature for 15 min before the NMR spectra were recorded. All spectroscopic data clearly show the formation of the corresponding cationic species:  $(2\text{-Ph-Ind})_2\text{ZrMe}^+\text{MeB}(\text{C}_6\text{F}_5)_3^-$  (**7**). No decomposition was detected when a toluene solution of **7** was left in the NMR tube over a period of 24 h at room temperature.

<sup>1</sup>H NMR ( $\text{C}_7\text{D}_8$ ,  $23\text{ }^{\circ}\text{C}$ ) for **7**:  $\delta$  7.11 (m, 6H), 7.00 (m, 4H), 6.82 (s, br. 2H), 6.68 (s, br. 2H), 6.62 (m, 4H), 6.09 (s, br. 2H), 5.85 (s, br. 2H),  $-0.37$  (s, 3H,

Zr-Me),  $-0.40$  (s, br. 3H, B-Me). <sup>19</sup>F NMR ( $\text{C}_7\text{D}_8$ ,  $23\text{ }^{\circ}\text{C}$ ):  $\delta$   $-132.60$  (d,  $^3J_{\text{F-F}} = 22.6\text{ Hz}$ , 6F, *o*-F),  $-159.78$  (t,  $^3J_{\text{F-F}} = 19.7\text{ Hz}$ , 3F, *p*-F),  $-164.75$  (m, 6F, *m*-F).

The above reaction was repeated but with a 2:1 Zr:B ratio. The formation of a small amount of the  $\mu$ -Me-bridged dinuclear cation,  $[(2\text{-Ph-Ind})_2\text{ZrMe}(\mu\text{-Me})\text{MeZr}(2\text{-Ph-Ind})_2]^+\text{MeB}(\text{C}_6\text{F}_5)_3^-$  (**8**), was apparent:  $-1.14$  (s, 6H, Zr-Me),  $-1.79$  (s, 3H, Zr-Me-Zr); other spectral data for **8** are similar to those of the monomeric cation **7**. There were no observable spectral changes between 20 min and 24 h of reaction time, and thus an equilibrium has been reached, resulting in a molar ratio of **7/8** = 10/1 in the mixture still containing excess, unreacted dimethyl precursor **2**.

## 2.3. General polymerization procedures

Polymerizations were performed either in 30-mL, oven- and flame-dried vacuum flasks inside the glovebox, or in 25-mL oven- and flame-dried Schlenk flasks interfaced to a dual-manifold Schlenk line. In a typical procedure, a metallocene complex (or a complex mixture in a desired ratio) and an activator in a predetermined ratio (see polymerization tables for details) were loaded into the flask in the glovebox. Toluene was added (10 mL total volume) and the mixture was stirred for 10 min to generate the active, cationic catalysts. MMA (1.00 mL, 9.35 mmol) was quickly added via pipette (for polymerizations in the glovebox) or gastight syringe (for polymerizations on the Schlenk line), and the sealed flask was kept with vigorous stirring at the pre-equilibrated bath temperature. After the measured time interval, the polymerization was quenched by the addition of 5 mL of 5% HCl-acidified methanol. The quenched mixture was precipitated into 100 mL of methanol, stirred for >1 h, filtered, washed with methanol, and dried in a vacuum oven at  $50\text{ }^{\circ}\text{C}$  overnight to a constant weight.

## 2.4. Polymer characterizations

Glass transition temperatures ( $T_g$ ) of the polymers were measured by differential scanning calorimetry (DSC) on a DSC 2920, TA Instrument. Samples were first heated to  $180\text{ }^{\circ}\text{C}$  at  $20\text{ }^{\circ}\text{C}/\text{min}$ , equilibrated at this temperature for 4 min, and cooled to  $0\text{ }^{\circ}\text{C}$  at  $20\text{ }^{\circ}\text{C}/\text{min}$ . After being held at this temperature for 4 min, the samples were then reheated to  $200\text{ }^{\circ}\text{C}$  at  $10\text{ }^{\circ}\text{C}/\text{min}$ . All  $T_g$  values were obtained from the second scan, after removing the thermal history. Polymer molecular weights and molecular weight distributions were measured by gel permeation chromatography (GPC) analyses carried out at  $40\text{ }^{\circ}\text{C}$ , a flow rate of  $1.0\text{ mL}/\text{min}$ , and with THF as the eluent, on a Waters University 1500 GPC instrument or a Polymer Laboratory-210 instrument. The instrument was calibrated with 10 PMMA

or PS standards, and chromatograms were processed with Waters Empower software.  $^1\text{H}$  NMR spectra for the analysis of PMMA microstructures were recorded in  $\text{CDCl}_3$  and analyzed according to the literature [23].

### 3. Results and discussion

#### 3.1. MMA polymerization using oscillating metallocene catalysts **1** and **2**

Results of MMA polymerization by **1** and **2** in toluene at 23 °C are summarized in Table 1. As shown in Table 1, polymerizations of MMA by the chloride **1** in a  $[\text{MMA}]/[\text{MMAO}]/[\text{I}]$  ratio of 1000/500/1 are sluggish; the isolated polymer yields were only 6% for a 2-h reaction (run 1) and 17% for a 24-h reaction (run 2). The PMMAs produced have low molecular weights ( $M_n < 10.2$  kg/mol) and broad molecular weight distributions ( $\text{PDI} = M_w/M_n > 1.48$ ), indicative of an uncontrolled polymerization. More importantly, the polymers produced are atactic with typical methyl triad distributions of  $[mm] = 30.3\%$ ,  $[mr] = 45.8\%$ , and  $[rr] = 23.9\%$  (run 1); this tacticity is also consistent with a measured  $T_g$  value of 97 °C for a typical atactic PMMA sample.

A large excess of MMAO and related alkyl aluminoxane activators present in MMA polymerizations can complicate the polymerization results, especially with a long reaction time, because alkyl aluminoxanes have been found to slowly polymerize MMA to PMMA with large PDI values [24]. To avoid any potential complications brought about by MMAO, we subsequently employed  $\text{B}(\text{C}_6\text{F}_5)_3$  and  $\text{Ph}_3\text{CB}(\text{C}_6\text{F}_5)_4$  activators for MMA polymerizations by the dimethyl catalyst precursor **2** because neither activator itself is capable of polymerizing MMA. The reaction of **2** and  $\text{B}(\text{C}_6\text{F}_5)_3$  (1:1 ratio) in toluene cleanly and quantitatively generates

the corresponding cationic species:  $(2\text{-Ph-Ind})_2\text{ZrMe}^+\text{MeB}(\text{C}_6\text{F}_5)_3^-$  (**7**, see Section 2). On the other hand, the same reaction but with a  $2/\text{B}(\text{C}_6\text{F}_5)_3$  ratio of 2/1 produces a mixture containing both the monomeric cation **7** and the dinuclear cation  $[(2\text{-Ph-Ind})_2\text{ZrMe}(\mu\text{-Me})\text{MeZr}(2\text{-Ph-Ind})_2]^+\text{MeB}(\text{C}_6\text{F}_5)_3^-$  (**8**). When the equilibrium was reached, the molar ratio of **7/8** in the mixture was approximately 10/1, and thus the monocation **7** is and the neutral dimethyl **2** are predominate species in the mixture.

Following the lead of this catalyst activation study, we carried out MMA polymerizations using **2** via in situ activation with  $\text{B}(\text{C}_6\text{F}_5)_3$  (runs 3 and 4) and with  $\text{Ph}_3\text{CB}(\text{C}_6\text{F}_5)_4$  (runs 5 and 6). As can be seen in Table 1, the polymerization of MMA by the dimethyl **2** in a  $[\text{MMA}]/[\text{2}]/[\text{B}(\text{C}_6\text{F}_5)_3]$  ratio of 400/1/1 is as sluggish as the polymerization using **1** via in situ activation with MMAO. The isolated polymer yield was only 4% for a 2-h reaction (run 3), but the PMMA produced has a moderate molecular weight of  $M_n = 32.4$  kg/mol and a broad molecular weight distribution of  $\text{PDI} = 1.67$ , giving a low initiator efficiency  $I^*$  ( $I^* = M_n(\text{calcd})/M_n(\text{exptl})$ , where  $M_n(\text{calcd}) = \text{MW}(\text{MMA}) \times [\text{MMA}]/[\text{2}] \times \text{conversion}\%$ ) of only 5%. All results indicate an uncontrolled polymerization under these conditions; however, the PMMA produced is syndio-rich atactic ( $[rr] = 65.8\%$ ).

The MMA polymerization, using a  $[\text{MMA}]/[\text{2}]/[\text{B}(\text{C}_6\text{F}_5)_3]$  ratio of 400/2/1 (run 2), afforded an 88% polymer yield in a 24 h time period, producing PMMA with a slightly higher syndiotacticity ( $[rr] = 69.6\%$ ); the measured  $T_g$  value of 128 °C is consistent with this tacticity. Significantly, the experimentally determined  $M_n$  of 32.4 kg/mol is approximately double what might be expected on the basis of a monomer-to-initiator  $\{[\text{MMA}]/[\text{2}]\}$  ratio of 200 and a monomer conversion value of 88% (i.e., the calculated  $M_n = 17.6$  kg/mol),

Table 1  
Results of MMA polymerization by  $(2\text{-Ph-Ind})_2\text{ZrX}_2$  ( $\text{X} = \text{Cl}$ , **1**;  $\text{Me}$ , **2**)<sup>a</sup>

Run no.	$[\text{Zr}]_0$ (mM)	$[\text{Cocatalyst}]_0$ (mM)	Time (h)	Yield (%)	$[mm]^b$ (%)	$[mr]^b$ (%)	$[rr]^b$ (%)	$T_g^c$ (°C)	$10^4 M_n^d$ (g/mol)	$\text{PDI}^d$ ( $M_w/M_n$ )
1	<b>1</b>	MMAO	2	6	30.3	45.8	23.9	97	1.02	1.48
	1.87	935								
2	<b>1</b>	MMAO	24	17	23.7	41.6	34.7	93	0.74	1.50
	1.87	935								
3	<b>2</b>	$\text{B}(\text{C}_6\text{F}_5)_3$	2	4	6.2	27.9	65.9	–	3.24	1.67
	4.68	4.68								
4	<b>2</b>	$\text{B}(\text{C}_6\text{F}_5)_3$	24	88	3.2	27.2	69.6	128	3.24	1.13
	9.36	4.68								
5	<b>2</b>	$\text{Ph}_3\text{CB}(\text{C}_6\text{F}_5)_4$	2	3	6.8	27.5	65.7	–	3.12	1.43
	4.68	4.68								
6	<b>2</b>	$\text{Ph}_3\text{CB}(\text{C}_6\text{F}_5)_4$	24	69	2.4	23.3	74.3	128	3.19	1.15
	9.36	4.68								

<sup>a</sup> All polymerizations were carried out in 5 mL toluene at 23 °C;  $[\text{MMA}] = 1.87$  M.

<sup>b</sup> Tacticity (methyl triad distributions) determined by  $^1\text{H}$  NMR spectroscopy in  $\text{CDCl}_3$ .

<sup>c</sup> Glass transition temperature ( $T_g$ ) determined by DSC from second scans.

<sup>d</sup> Number-average molecular weight ( $M_n$ ) and polydispersity index (PDI) determined by GPC relative to PMMA standards.

giving a much improved initiator efficiency of 54%. This evidence, coupled with a low PDI value of 1.13, argues that the polymerization using a 2:1 ratio of **2**/ $\text{B}(\text{C}_6\text{F}_5)_3$  occurs via a *bimetallic mechanism* [1j] and is *controlled*. Results of the MMA polymerization by **2** activated with  $\text{Ph}_3\text{CB}(\text{C}_6\text{F}_5)_4$  are similar to those obtained from **2** activated with  $\text{B}(\text{C}_6\text{F}_5)_3$ , with only small variations in polymer yield, as well as in PMMA tacticity, molecular weight, and polydispersity values.

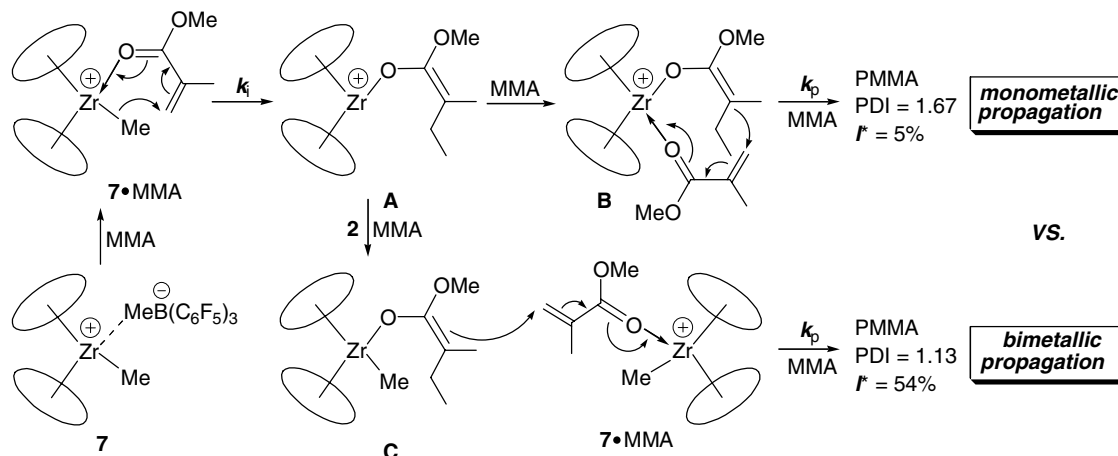
The observed sharply different MMA polymerization behavior between the 1:1 **2**/ $\text{B}(\text{C}_6\text{F}_5)_3$  and 2:1 **2**/ $\text{B}(\text{C}_6\text{F}_5)_3$  systems can be explained by the competition between the monometallic and bimetallic propagation mechanisms shown in Scheme 2. In the MMA polymerization by a 1:1 ratio of **2**/ $\text{B}(\text{C}_6\text{F}_5)_3$ , which clearly generates the cation **7**, a slow initiation step involves methyl transfer to the coordinated MMA in the  $7 \cdot \text{MMA}$  adduct, leading to cationic zirconocene enolate **A** [1j]. Subsequent events involve MMA binding to **A** and repeated *intramolecular* Michael additions involved in **B** and its homologues in propagation steps, producing PMMA via a monometallic propagation mechanism. On the other hand, in the MMA polymerization by a 2:1 ratio of **2**/ $\text{B}(\text{C}_6\text{F}_5)_3$ , which affords a mixture containing predominately the monocation **7** and the unreacted neutral dimethyl **2**, a fast methyl transfer reaction between **A** and **2** produces neutral methyl zirconocene enolate **C** [1j] and **7** (which is then trapped by MMA in the form of the  $7 \cdot \text{MMA}$  adduct). (The dinuclear cation **8** can be considered as the precursor of  $7 \cdot \text{MMA}$  and **2** in the presence of MMA [21].) Subsequent events involve rapidly repeated *intermolecular* Michael additions of **C** and its homologues to  $7 \cdot \text{MMA}$  in propagation steps, leading to PMMA via a bimetallic propagation mechanism. For the present unbridged bis(indenyl) zirconocene system, it is clear that the bimetallic pathway is more competitive and controlled than a monometallic one, the result of which is consistent with that obtained from the parent  $[\text{Cp}_2\text{Zr}]$  system [1a].

### 3.2. MMA polymerization using mixtures of diastereomeric metallocene catalysts

Table 2 summarizes the results of MMA polymerizations by mixtures of diastereomeric zirconocenes **3** and **4** in toluene at 25 °C. As can be seen in Table 2, the polymerization of MMA by pure *rac*-**3**, activated with  $\text{B}(\text{C}_6\text{F}_5)_3$ , produces isotactic PMMA ( $[mm] = 90.4\%$ ) with a low PDI value of 1.12 and occurs via an enantiomeric-site control mechanism  $\{[2[rr]/[mr] = 0.95, \text{run } 1]\}$ . On the other hand, diastereomeric mixtures with *rac/meso* ratios = 1/1 (run 2), 1/3.5 (run 3), and 1/8.7 (run 4) afford bimodal polymers (Fig. 1), and the isotacticity, in terms of the  $[mm]$  values, decreases as the *meso*-isomer content is increased.

Interestingly, pure *meso*-diastereomers themselves, *meso*-**3** (run 5) and *meso*-**4** (run 6), produce bimodal, syndio-rich atactic PMMAs. We first suspected that the *meso*-diastereomers used for the polymerization studies were perhaps contaminated with a trace amount of the *rac*-diastereomer; however,  $^1\text{H}$  NMR spectra (Fig. 2) of the *meso*-diastereomer showed a complete absence of the *rac*-diastereomer. Thus, the formation of bimodal polymers using *meso*-diastereomers is presumably attributed to the co-existence of two independent polymerization processes (i.e., monometallic mechanism vs bimetallic mechanism). On basis of the same reasoning, the diastereomeric mixtures containing various percentages of the *meso*-diastereomer will also produce bimodal polymers, as was observed here.

It is worth noting that, when activated with  $\text{Al}(\text{C}_6\text{F}_5)_3$  instead of  $\text{B}(\text{C}_6\text{F}_5)_3$ , the same *meso*-diastereomers, diastereomeric mixtures, or *rac*-diastereomers uniformly produce unimodal, syndiotactic PMMA via a chain-end control mechanism (runs 7–10). This phenomena is due to the fact that the  $\text{Al}(\text{C}_6\text{F}_5)_3$ -activated MMA polymerization involves a bimetallic polymerization mechanism via anionic enolaluminum propagating



Scheme 2.

Table 2  
Results of MMA polymerization by mixtures of diastereomeric zirconocenes<sup>a</sup>

Run no.	Catalyst ( <i>rac/meso</i> ratio)	Activator (Zr/B = 1/1)	Yield (%)	$M_n^b$ (kg/mol)	PDI <sup>b</sup> ( $M_w/M_n$ )	[ <i>mm</i> ] <sup>c</sup> (%)	[ <i>mr</i> ] <sup>c</sup> (%)	[ <i>rr</i> ] <sup>c</sup> (%)	2[ <i>rr</i> ]/[ <i>mr</i> ]	$P_{m/r} + P_{r/m}^d$
1	<b>3</b> (1:0)	B(C <sub>6</sub> F <sub>5</sub> ) <sub>3</sub>	>99	28.4	1.12	90.4	6.5	3.1	0.95	0.55
2	<b>3</b> (1:1)	B(C <sub>6</sub> F <sub>5</sub> ) <sub>3</sub>	>99	30.8	bimodal	86.3	7.8	5.9	–	–
3	<b>3</b> (1:3.5)	B(C <sub>6</sub> F <sub>5</sub> ) <sub>3</sub>	92	28.8	bimodal	70.9	13.6	15.5	–	–
4	<b>3</b> (1:8.7)	B(C <sub>6</sub> F <sub>5</sub> ) <sub>3</sub>	85	29.4	bimodal	56.5	17.9	25.6	–	–
5	<b>3</b> (0:1)	B(C <sub>6</sub> F <sub>5</sub> ) <sub>3</sub>	75	16.7	bimodal	11.5	33.1	55.4	–	–
6	<b>4</b> (0:1)	B(C <sub>6</sub> F <sub>5</sub> ) <sub>3</sub>	>99	20.5	bimodal	12.0	36.3	51.7	–	–
7	<b>3</b> (1:0)	Al(C <sub>6</sub> F <sub>5</sub> ) <sub>3</sub>	>99	28.8	1.19	4.3	35.1	60.6	3.45	1.02
8	<b>3</b> (1:1)	Al(C <sub>6</sub> F <sub>5</sub> ) <sub>3</sub>	>99	25.6	1.36	4.6	35.8	59.6	3.33	1.03
9	<b>3</b> (0:1)	Al(C <sub>6</sub> F <sub>5</sub> ) <sub>3</sub>	>99	27.9	1.28	3.5	32.1	64.4	4.01	1.02
10	<b>4</b> (0:1)	Al(C <sub>6</sub> F <sub>5</sub> ) <sub>3</sub>	>99	37.6	1.30	2.8	32.3	64.9	4.02	1.06

<sup>a</sup> Polymerization conditions: 46.7 μmol Zr; molar ratio [MMA]/[Zr]/[B] = 200:1:1; 10 mL toluene; 25 °C; 2 h.

<sup>b</sup> Determined by GPC relative to PMMA (entries 1, 7, and 9–10) or PS (entries 2–6, and 8) standards.

<sup>c</sup> Determined by <sup>1</sup>H NMR spectroscopy.

<sup>d</sup>  $P_{m/r}$  is the probability that the monomer adds in racemo fashion to a meso chain end and  $P_{r/m}$  is the probability that the monomer adds in meso fashion to a racemo chain end.

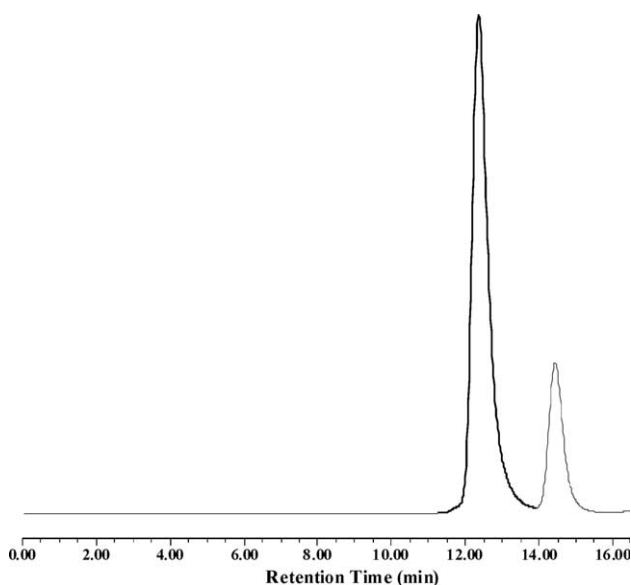


Fig. 1. A typical GPC trace showing a bimodal distribution of PMMA produced by *meso*-diastereomers or diastereomeric mixtures.

centers, and the metallocene cation derived from methyl transfer of the Zr–Me moiety to the alane-activated MMA in the initiation step functions only as a charge-compensating cation [2i,4a,5a,25]. As a result, the char-

acteristics of the MMA polymerization activated by Al(C<sub>6</sub>F<sub>5</sub>)<sub>3</sub> are independent of the type of metallocene precursors used.

### 3.3. MMA polymerization using diastereospecific metallocene pairs

We also probed a third strategy for the possible production of stereoblock PMMA – use of diastereospecific metallocene catalyst pairs, the results of which are summarized in Table 3. Chiral, *C*<sub>2</sub>-symmetric *rac*-**4** is highly isospecific [2], whereas achiral *C*<sub>2v</sub>-symmetric **5** [2i] and *C*<sub>s</sub>-symmetric **6** [6a] produce syndio-rich atactic and syndiotactic PMMA, respectively. We reasoned that, if the growing diastereomeric polymer chains, derived from the diastereospecific catalyst centers in the MMA polymerization using a diastereospecific metallocene pair (e.g., *rac*-**4**/**5** or *rac*-**4**/**6** pair), can undergo infrequent exchange between the two diastereospecific catalyst sites, then stereoblock microstructures could be generated.

As can be seen from Table 3, however, all polymerizations using the *rac*-**4**/**5** pair in various ratios consistently produce only isotactic PMMA (runs 1–4); a mixture containing a large excess of **5** yield PMMA with a broad molecular weight distribution (PDI = 2.66, run 5). The characteristics of the polymerization with the

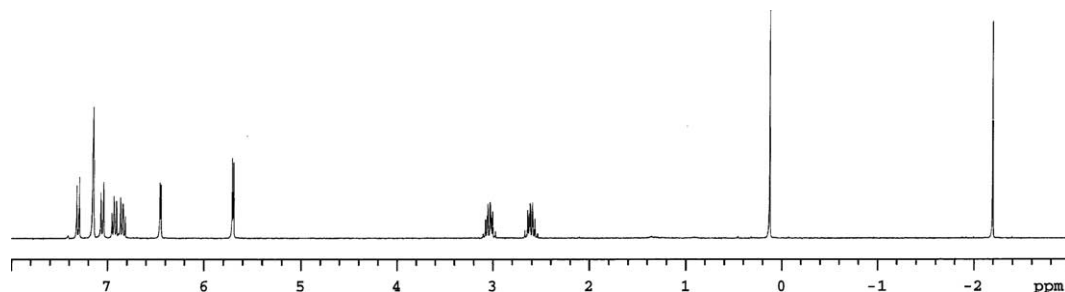


Fig. 2. <sup>1</sup>H NMR spectrum of pure *meso*-(EBI)ZrMe<sub>2</sub> (C<sub>6</sub>D<sub>6</sub>).

Table 3  
Results of MMA polymerization by diastereospecific catalyst pairs<sup>a</sup>

Run no.	[cat1] (mM)	cat2 [cat1]:[cat2]	[MMA]:[cat1]	Yield (%)	$M_n^b$ (kg/mol)	PDI <sup>b</sup> ( $M_w/M_n$ )	[ <i>mm</i> ] <sup>c</sup> (%)	[ <i>mr</i> ] <sup>c</sup> (%)	[ <i>rr</i> ] <sup>c</sup> (%)
1	<i>rac</i> - <b>4</b> (3.11)	<b>5</b> (2:1)	300:1	>99	59.7	1.18	94.0	3.7	2.3
2	<i>rac</i> - <b>4</b> (2.34)	<b>5</b> (1:1)	400:1	>99	76.8	1.18	95.4	2.8	1.8
3	<i>rac</i> - <b>4</b> (1.56)	<b>5</b> (1:2)	600:1	>99	112	1.21	94.4	3.0	2.6
4	<i>rac</i> - <b>4</b> (1.17)	<b>5</b> (1:1)	800:1	>99	134	1.16	94.4	3.5	2.1
5	<i>rac</i> - <b>4</b> (0.66)	<b>5</b> (1:6)	1400:1	72	100	2.66	90.6	3.9	5.5
6	<i>rac</i> - <b>4</b> (2.34)	<b>6</b> (1:1)	400:1	>99	77.1	1.16	96.0	2.5	1.5
7	<i>rac</i> - <b>4</b> (1.56)	<b>6</b> (1:2)	600:1	>99	108	1.14	95.7	2.6	1.7
8	<i>rac</i> - <b>4</b> (1.17)	<b>6</b> (1:1)	800:1	>99	161	1.12	97.1	1.9	1.0
9	<i>rac</i> - <b>4</b> (0.78)	<b>6</b> (1:2)	1200:1	>99	260	1.09	96.2	2.5	1.3

<sup>a</sup> Polymerization conditions: molar ratio [(cat1 + cat2)/[B(C<sub>6</sub>F<sub>5</sub>)<sub>3</sub>]] = 1:1; 10 mL toluene; 23 °C; 2 h.

<sup>b</sup> Number-average molecular weight ( $M_n$ ) and polydispersity index (PDI) determined by GPC relative to PMMA standards.

<sup>c</sup> Methyl triad distributions determined by <sup>1</sup>H NMR spectroscopy.

*rac*-**4/6** pair are similar to those observed for the *rac*-**4/5** pair. Thus, under the conditions employed in the present study, the isospecific site for both diastereospecific pairs dominates the polymerization events, and the aspecific (i.e. **5**) and syndiospecific (i.e. **6**) sites are largely nonproductive.

#### 4. Conclusions

To probe new strategies for the production of stereoblock PMMA, we have investigated the behavior of the MMA polymerization using three classes of group 4 metallocene catalysts, including oscillating catalysts **1** and **2**, mixtures of diastereomeric zirconocene catalysts **3** and **4**, as well as diastereospecific catalyst pairs *rac*-**4/5** and *rac*-**4/6**. These three systems were chosen for this study because of their potential for exhibiting either catalyst-site isomerization within the timescale of the MMA polymerization or exchange of growing diastereomeric polymer chains between diastereospecific catalyst sites.

Although none of the three systems investigated gave the desired stereoblock microstructures, several findings of this study are significant. First, the MMA polymerization with a 2/1 ratio of **2**/B(C<sub>6</sub>F<sub>5</sub>)<sub>3</sub> or **2**/Ph<sub>3</sub>CB(C<sub>6</sub>F<sub>5</sub>)<sub>4</sub> – the reaction of which produces a mixture containing predominately the monocation **7** and the unreacted **2** – is controlled and produces syndiotactic PMMA, whereas the MMA polymerization using the monomeric cation alone is sluggish and uncontrolled. These results are consistent with the conclusion that the bimetallic propagating mechanism is more effective and controlled than the monometallic one for the MMA polymerization by the unbridged bis(indenyl) oscillating zirconocene catalysts.

Second, unlike pure *rac*-diastereomers, upon activation with B(C<sub>6</sub>F<sub>5</sub>)<sub>3</sub>, pure *meso*-diastereomers yield bimodal polymers. The formation of bimodal polymers with *meso*-diastereomers suggests that the *meso*-orientation

of the bridged indenyl phenyl rings likely effects a competition between two independent polymerization processes – monometallic mechanism vs. bimetallic mechanism.

Third, the isospecific catalyst site dominates the polymerization events in the MMA polymerization using diastereospecific metallocene catalyst pairs, while the aspecific and syndiospecific sites are largely nonproductive. This phenomena is, of course, catalyst concentration-dependent. One can reasonably assume that, under suitable polymerization conditions, both catalyst sites in a diastereospecific catalyst mixture can be simultaneously turned on. If such conditions are met, then the question becomes: can growing diastereomeric polymer chains exchange between two cationic, diastereospecific catalyst sites? Research to answer this question is currently underway.

#### Acknowledgements

This work was supported by the National Science Foundation and Colorado State University. We thank Boulder Scientific Co. for the gift of B(C<sub>6</sub>F<sub>5</sub>)<sub>3</sub>; Y.N. and M.J.C. thank Wesley Mariott and Andrew Bolig for their respective mentorship. E.Y.C. acknowledges an Alfred P. Sloan Research Fellowship.

#### References

- [1] (a) G. Stojcevic, H. Kim, N.J. Taylor, T.B. Marder, S. Collins, *Angew. Chem. Int. Ed.* 43 (2004) 5523–5526;  
(b) B. Lian, L. Toupet, J.-F. Carpentier, *Chem. Eur. J.* 10 (2004) 4301–4307;  
(c) M. Ferenz, F. Bandermann, R. Sustmann, W. Sicking, *Macromol. Chem. Phys.* 205 (2004) 1196–1205;  
(d) G. Karanikolopoulos, C. Batis, M. Pitsikalis, N. Hadjichristidis, *J. Polym. Sci. Part A: Polym. Chem.* 42 (2004) 3761–3774;  
(e) J. Wang, G. Odian, H. Haubenstock, *Polym. Prepr. Am. Chem. Soc. Div. Polym. Chem.* 44 (2003) 673–674;

- J. Wang, H. Haubenstock, G. Odian, *Polym. Prepr. Am. Chem. Soc. Div. Polym. Chem.* 44 (2003) 675–676;
- (f) F. Bandermann, M. Ferez, R. Sustmann, W. Sicking, *Macromol. Symp.* 174 (2001) 247–253;
- (g) G. Karanikolopoulos, C. Batis, M. Pitsikalis, N. Hadjichristidis, *Macromolecules* 34 (2001) 4697–4705;
- (h) F. Bandermann, M. Ferez, R. Sustmann, W. Sicking, *Macromol. Symp.* 161 (2000) 127–134;
- (i) T. Shiono, T. Saito, N. Saegusa, H. Hagihara, T. Ikeda, H. Deng, K. Soga, *Macromol. Chem. Phys.* 199 (1998) 1573–1579;
- (j) Y. Li, D.G. Ward, S.S. Reddy, S. Collins, *Macromolecules* 30 (1997) 1875–1883;
- (k) H. Deng, T. Shiono, K. Soga, *Macromol. Chem. Phys.* 196 (1995) 1971–1980;
- (l) S. Collins, D.G. Ward, *J. Am. Chem. Soc.* 114 (1992) 5460–5462;
- (m) W.B. Farnham, W. Hertler, US Pat. (1988) 4,728,706.
- [2] (a) A.D. Bolig, E.Y.-X. Chen, *J. Am. Chem. Soc.* 126 (2004) 4897–4906;
- (b) J.W. Strauch, J.-L. Fauré, S. Bredeau, C. Wang, G. Kehr, R. Fröhlich, H. Luftmann, G. Erker, *J. Am. Chem. Soc.* 126 (2004) 2089–2104;
- (c) E.Y.-X. Chen, M.J. Cooney, *J. Am. Chem. Soc.* 125 (2003) 7150–7151;
- (d) G. Karanikolopoulos, C. Batis, M. Pitsikalis, N. Hadjichristidis, *Macromol. Chem. Phys.* 204 (2003) 831–840;
- (e) C. Batis, G. Karanikolopoulos, M. Pitsikalis, N. Hadjichristidis, *Macromolecules* 36 (2003) 9763–9774;
- (f) See [1e];
- (g) A.D. Bolig, E.Y.-X. Chen, *J. Am. Chem. Soc.* 124 (2002) 5612–5613;
- (h) H. Frauenrath, H. Keul, H. Höcker, *Macromolecules* 34 (2001) 14–19;
- (i) A.D. Bolig, E.Y.-X. Chen, *J. Am. Chem. Soc.* 123 (2001) 7943–7944;
- (j) P.A. Cameron, V. Gibson, A.J. Graham, *Macromolecules* 33 (2000) 4329–4335;
- (k) T. Stuhldreier, H. Keul, H. Höcker, *Macromol. Rapid Commun.* 21 (2000) 1093–1098;
- (l) Y.X. Chen, M.V. Metz, L. Li, C.L. Stern, T.J. Marks, *J. Am. Chem. Soc.* 120 (1998) 6287–6305;
- (m) H. Deng, T. Shiono, K. Soga, *Macromolecules* 28 (1995) 3067–3073;
- (n) K. Soga, H. Deng, T. Yano, T. Shiono, *Macromolecules* 27 (1994) 7938–7940;
- (o) S. Collins, D.G. Ward, K.H. Suddaby, *Macromolecules* 27 (1994) 7222–7224.
- [3] (a) N. Saegusa, T. Shiono, T. Ikeda, K. Mikami, (1998) JP 10330391;
- (b) See [1m].
- [4] (a) J. Jin, W.R. Mariott, E.Y.-X. Chen, *J. Polym. Chem. Part A: Polym. Chem.* 41 (2003) 3132–3142;
- (b) J. Jin, E.Y.-X. Chen, *Organometallics* 21 (2002) 13–15.
- [5] (a) E.Y.-X. Chen, *J. Polym. Sci. Part A: Polym. Chem.* 42 (2004) 3395–3403;
- (b) T.R. Jensen, S.C. Yoon, A.K. Dash, L. Luo, T.J. Marks, *J. Am. Chem. Soc.* 125 (2003) 14482–14494.
- [6] (a) A. Rodriguez-Delgado, W.R. Mariott, E.Y.-X. Chen, *Macromolecules* 37 (2004) 3092–3100;
- (b) J. Jin, E.Y.-X. Chen, *Macromol. Chem. Phys.* 203 (2002) 2329–2333;
- (c) J. Jin, D.R. Wilson, E.Y.-X. Chen, *Chem. Commun.* (2002) 708–709;
- (d) H. Nguyen, A.P. Jarvis, M.J.G. Lesley, W.M. Kelly, S.S. Reddy, N.J. Taylor, S. Collins, *Macromolecules* 33 (2000) 1508–1510.
- [7] (a) M. Hölscher, H. Keul, H. Höcker, *Macromolecules* 35 (2002) 8194–8202;
- (b) M. Hölscher, H. Keul, H. Höcker, *Chem. Eur. J.* 7 (2001) 5419–5426;
- (c) R. Sustmann, W. Sicking, F. Bandermann, M. Ferez, *Macromolecules* 32 (1999) 4204–4213.
- [8] G.W. Coates, R.M. Waymouth, *Science* 267 (1995) 217–219.
- [9] R.D. Allen, T.E. Long, J.E. McGrath, *Polym. Bull.* 15 (1986) 127–134.
- [10] (a) J.C.W. Chien, W.-M. Tsai, M.D. Rausch, *J. Am. Chem. Soc.* 113 (1991) 8570–8571;
- (b) J.A. Ewen, M.J. Elder, *Eur. Pat. Appl. EP* (1991) 0,426,637.
- [11] S. Feng, G.R. Roof, E.Y.-X. Chen, *Organometallics* 21 (2002) 832–839.
- [12] (a) P. Biagini, G. Lugli, L. Abis, P. Andreussi, US Pat. (1997) 5,602,269;
- (b) C.H. Lee, S.J. Lee, J.W. Park, K.H. Kim, B.Y. Lee, J.S. Oh, *J. Mol. Catal. A: Chem.* 132 (1998) 231–239.
- [13] G.W. Coates, R.M. Waymouth, E.M. Hauptman, US Pat. (1997) 5,594,080.
- [14] J.N. Christopher, G.M. Diamond, R.F. Jordan, J.L. Petersen, *Organometallics* 15 (1996) 4038–4044.
- [15] G.M. Diamond, R.F. Jordan, J.L. Petersen, *J. Am. Chem. Soc.* 118 (1996) 8024–8033.
- [16] E. Samuel, M.D. Rausch, *J. Am. Chem. Soc.* 95 (1973) 6263–6267.
- [17] J.C. Stevens, F.J. Timmers, D.R. Wilson, G.F. Schmidt, P.N. Nickias, R.K. Rosen, G.W. Knight, S. Lai, *Eur. Pat. Appl.* (1991) EP 0 416 815 A2.
- [18] W.A. Herrmann, J. Rohrmann, E. Herdtweck, W. Spaleck, A. Winter, *Angew. Chem. Int. Ed. Engl.* 28 (1989) 1511–1512.
- [19] D. Balboni, I. Camurati, G. Prini, L. Resconi, S. Galli, P. Mercandelli, A. Sironi, *Inorg. Chem.* 40 (2001) 6588–6597.
- [20] E.Y.-X. Chen, W.J. Kruper, G. Roof, D.R. Wilson, *J. Am. Chem. Soc.* 123 (2001) 745–746.
- [21] X. Yang, C.L. Stern, T.J. Marks, *J. Am. Chem. Soc.* 116 (1994) 10015–10031.
- [22] Y.-X. Chen, T.J. Marks, *Organometallics* 16 (1997) 3649–3657.
- [23] (a) F.A. Bovey, P.A. Mirau, *NMR of Polymers*, Academic Press, San Diego, CA, 1996;
- (b) R.C. Ferguson, D.W. Ovenall, *Polym. Prepr. (Am. Chem. Soc. Div. Polym. Chem.)* 26 (1985) 182–183;
- (c) R. Subramanian, R.D. Allen, J.E. McGrath, T.C. Ward, *Polym. Prepr. (Am. Chem. Soc. Div. Polym. Chem.)* 26 (1985) 238–240.
- [24] B. Wu, R.W. Lenz, B. Hazer, *Macromolecules* 32 (1999) 6856–6859.
- [25] W.R. Mariott, L.M. Hayden, E.Y.-X. Chen, *ACS Symp. Ser.* 857 (2003) 101–111.